

Boron/Nitrogen Co-doped carbon quantum dots as a high sensitive and selective fluorescent sensor for PO_4^{3-} detection

Azadeh Ostad Chinigar^{ID}, Ashkan Shomali^{ID} and Hassan Valizadeh^{ID*}

Department of Chemistry, Azarbaijan Shahid Madani University, P.O. Box: 53714-161, Tabriz, Iran

(Received January 20, 2020; Revised March 25, 2020; Accepted March 27, 2020)

Abstract: Boron/Nitrogen doped carbon quantum dots (BNCQD) was synthesized and its physicochemical and optical properties were investigated by FT-IR, XRD, XPS, TEM and spectroscopic methods. The freshly prepared BNCQD shows a strong green fluorescence at 400 nm excitation, and PO_4^{3-} anion can readily turn-on the fluorescence of BNCQD through forming stable complex. Then, we designed a turn-on fluorescence sensor for phosphate ion detection which indicate a high selectivity towards PO_4^{3-} ions in comparison with the other anions with a limit of detection of 0.1 μM . It was approved that BNCQD is highly sensitive and selective to detect PO_4^{3-} anion in wastewater.

Keywords: B/N-carbon dots; phosphate; sensor ©2020 ACG Publications. All right reserved.

1. Introduction

Excessive presence of phosphorus species in drinking water and various types of agricultural, domestic, and industrial wastewaters is a serious problem worldwide.¹ Presence of excess phosphate into the aquatic environment leads to eutrophication which can promote growth of harmful algal and decrease the amount of dissolved oxygen in water.²

Therefore, decreasing or removing the phosphate in water is very important function for abbreviating the pollution of water bodies. Various techniques have been reported for phosphate removal successfully, such as chemical precipitation, adsorption, osmosis and biological treatment.³⁻⁶ High efficiency, simple operation and applicability at lower concentrations in adsorption technique, make it the most widely used method for phosphate removal.⁷

Therefore, trace level detection of phosphate is very beneficial from the point of view of water hygiene. There are many protocols containing doping, surface modifications, and their analytical developments have been reported.⁸⁻¹² Qiu et al used GQD combined with Europium ions as photoluminescent probes for phosphate sensing.¹³ Jin et al. reported the detection of phosphate ions using of phosphorescence of Mn doped ZnS quantum dots.¹⁴ Dan et al. used Ag₂S QD/metal – organic shell composite as a fluorescent sensor for the detection of Phosphate ion in aqueous solutions.¹⁵ Phosphate ion detection have also been reported using silver nanoclusters/metal–organic shell composite in aqueous solutions.¹⁶

* Corresponding authors: Email: hvalizadeh2@yahoo.com, Phone:+9833319301 ; Fax: +9834327522;

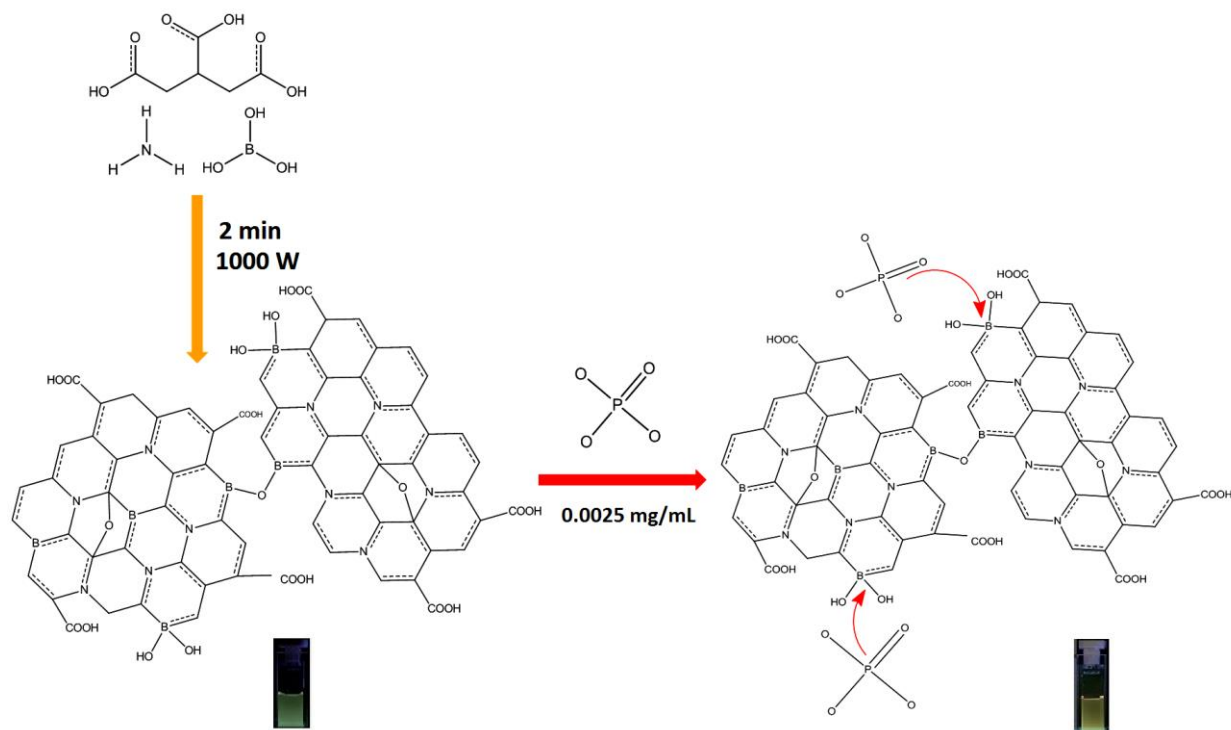
In continuation of our interest in preparation and using CQD and modified CQD as a reagent and/or catalyst in chemical reactions,¹⁷⁻¹⁹ we decided to prepare B-doped CQD and examine its applicability for the sensing of some important anions.

Due to their excellent optical and electronic properties, carbon quantum dots (CQD) are shown as a very interesting compounds from various areas including sensors, bioimaging and catalysis.²⁰⁻²² To overcome some drawbacks such as low quantum yields of pristine CQD, which contain only carbon and oxygen atoms, surface modification as well as doping with elements such as nitrogen was performed to achieve high fluorescence efficiency.²³⁻²⁶

Intrinsic properties of carbon materials are effectively tuned by doping with heteroatoms, and new phenomena and unexpected characteristics are produced. There are numerous reports on the doping in graphene by N and B substitution of C to properly change their structural, optical and chemical properties.²⁷⁻²⁹ Doping these heteroatoms in graphene makes it a semimetal or a semiconductor, with possible applications in sensing.³⁰⁻³¹

Some reported studies have shown that doping with nitrogen can largely improve the fluorescence of doped CQD.³²⁻³⁴ Surface modified and element-doped photoluminescence CQD were used as biocompatible, biodetectors and biosensors.³⁵ Liu et al reported the using of N-doped CQD as a glucose sensor.³⁶

Herein, we report an efficient fluorescence sensing system for phosphate anion detection based on the boron and nitrogen-doped graphene quantum dots (BNCQD), which was synthesized by using a one-pot MW-assisted simple reaction of boric acid, citric acid and ammonia in an aqueous solution. Phosphate is a fundamental component of the nutritional chain of aquatic microorganisms, and an appropriate indicator of organic pollution in water.³³ Therefore phosphate tracing is of great important for controlling of eutrophication. Scheme 1 shows the combination of BNCQD and phosphate and the principles of this anion detection concept. Fluorescence intensity is increased by the coordination of phosphate anion to the B atoms in the BNCQD.



Scheme 1. BNCQD preparation and the effect of phosphate absorption on its fluorescence intensity.

2. Experimental

2.1. General Information

All solvents and reagents are industrial and used without further purification. Infrared (FT-IR) spectra of samples in KBr were recorded by a Bruker PS-15 spectrometer. UV–Vis absorption spectrum was carried out using a UV/VIS/NIR spectrometer (Perkin Elmer lambda 650). The morphology of BNCQDs was observed on a Zeiss EM10C transmission electron microscope (TEM). Analysis of X-ray photoelectron spectroscopy (XPS) were done with an ESCALAB 250.Xi from Thermo Scientific using Mg X-ray resource. The structure of the nanoparticle was determined using X-ray diffraction pattern (XRD, Bruker, AXS model D8). Fluorescence spectra were measured on a Jasco FP-6500 fluorescence spectrophotometer. MW experiments were conducted in a Milestone MicroSynth apparatus.

2.2. Synthesis of BNCQD

Citric acid (1g, 0.052 mol), boric acid (0.125g, 0.0053 mol) and ammonia (0.80 mL, 18.66 mol) were added in 5mL water and stirred vigorously. Then the mixture was heated with full power MWI (1000 W) for 2 minutes. Then the dark-green reaction mixture was cooled to room temperature and deionized water (5 mL) was added and stirred thoroughly. Then, water was evaporated under the vacuum at 50 °C and the residual (BNCQD) was collected for further analysis.

2.3. Synthesis of NCQD

Citric acid (1 g, 0.052 mol) and ammonia (0.3 g, 0.017 mol) were add in 5mL water and heated with full power microwave (1000 W) for 3 minutes. The light brown liquid obtained was placed in oven under 50 °C temperature and NCQD were collected.

2.4. Experimental Conditions

For sensitivity examination, Na₃PO₄ solutions in deionized water were prepared in various concentrations (0.1–120 μM). Then, the resultant solution (5 mL) was added into the deionized aqueous solution of BNCQD (0.0025 mg/mL) at 25 °C with the pH range of 6-8 and immediately mixed thoroughly. After incubation for 10 min, the fluorescence spectrum of the resulting solution was recorded at $\lambda_{ex} = 400$ nm. Described procedure was carried out for all of other salts such as Na₂CO₃, KOH, NaOH, NaNO₃, HCN, Na₂SO₄, AcOH, HF, HCl, HBr and HI.

2.5. Measurement of the Quantum Yield

The quantum yield of the synthesized BNCQD and NCQD were determined according to below equation using quinine sulfate as a standard fluorescent.

$$Y_u = Y_{st} \left(\frac{I_u}{I_{st}} \right) \left(\frac{A_{st}}{A_u} \right) \left(n_u^2 n_{st}^{-2} \right)$$

In this equation Y is the quantum yield, I is the measured integrated emission intensity, n is the refractive index, and A is the extinction. The “u” and “st” are refered for sample with unknown QY and for standard respectively.

3. Results and Discussion

3.1. Characterization

B- and N-doped carbon quantum dots (BNCQD) was prepared under MW irradiation by using boric acid as the boron source and ammonia as the source of nitrogen (Step 1, Scheme 1). Transmission electron microscopy (TEM) image in Figure 1 shows that the particle size distribution of BNCQD is in the range of 5-30 nm and that the average size is approximately 15 nm.

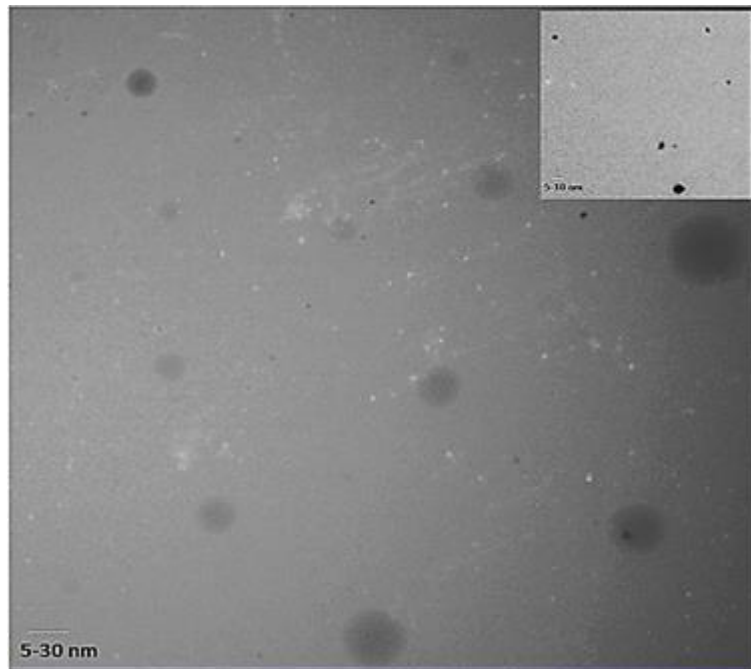


Figure 1. TEM image of BNCQD

Figure 2 shows the XRD pattern of the crystalline structure of BNCQD and exhibit a weak broad peak at around 22.0° belong to the (002) planes of CQD.³⁷⁻³⁸ the interlayer spacing of BNCQD was 3.82 Å which is larger in comparison with bulk graphite (3.34 Å). The further interlayer distance is related to the functional groups containing on the surface of BNCQD.

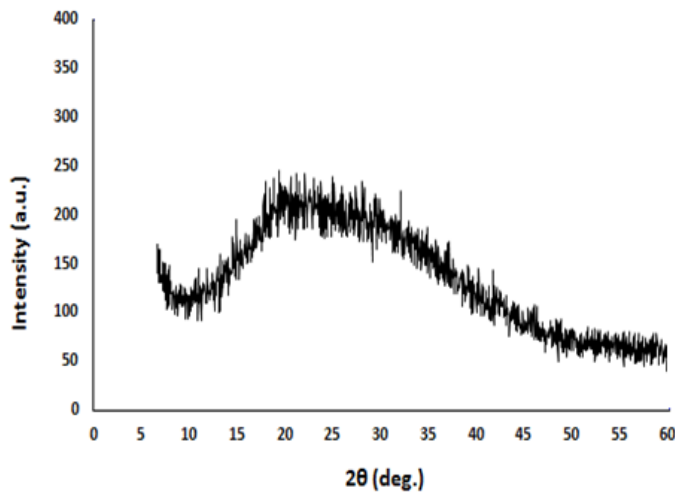


Figure 2. XRD pattern of BNCQD

XPS survey spectrum of BNCQD (Figure 3) shows the presence of C, O, N and B with atomic percentages of 32.73%, 57.34%, 8.73%, and 1.20% and the corresponding C1s, O1s, N1s, B1s peaks are located at ca. 286.74, 532.75, 401.11 and 192.44 eV, respectively. Therefore, the successful incorporation of B atoms into the CQD was confirmed. As shown in Figure 3b the high resolution C1s spectrum confirmed the O-rich groups, such as C–O/C–N, C=C and O–C=O. In the high resolution B1s spectrum (Figure 3d), the peaks at the range of 192–193 eV correspond to the B–C bonds present in BNCQD

structure. The presence of B–N and C–N bonds is also confirmed from the high resolution N1s spectrum (Figure 3e). The existence of C–B bonds in the BNCQD can be confirmed from the all these results.

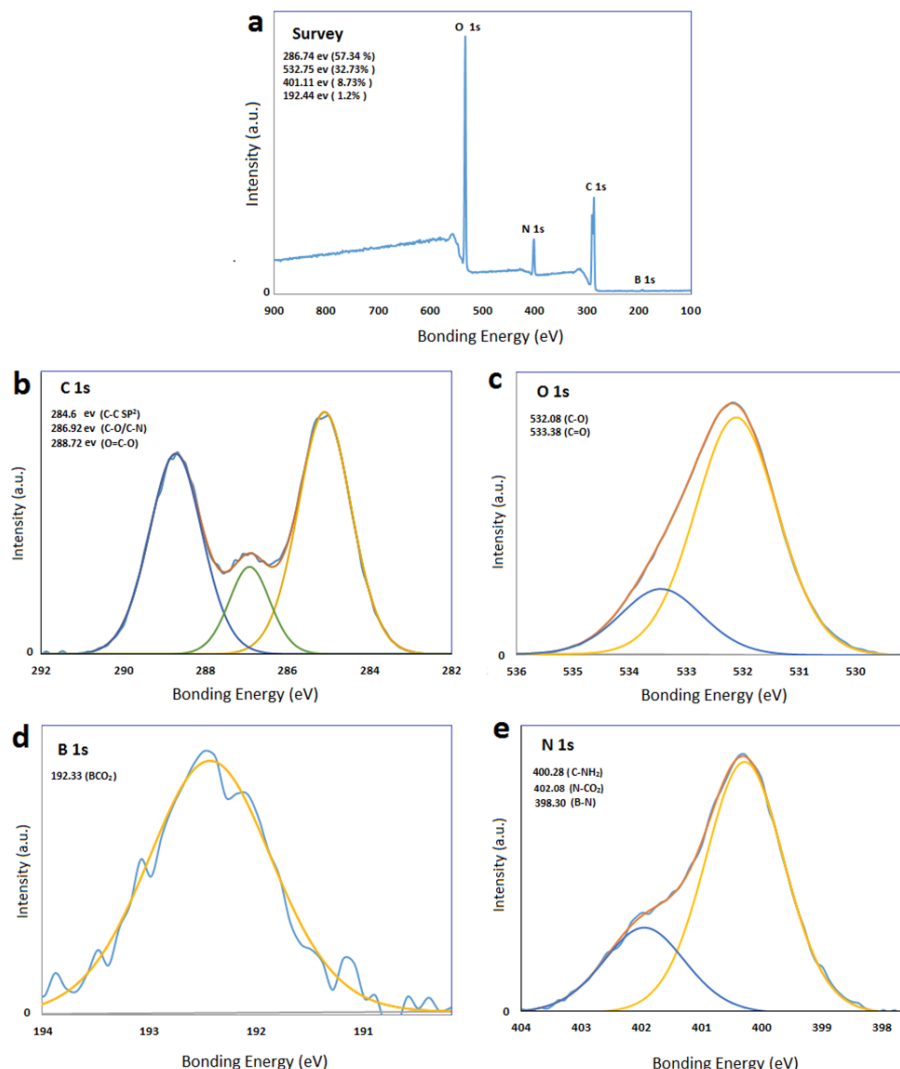


Figure 3. (a) X-ray photoelectron spectrum of BNCQD, (b) C1s spectrum, (c) O1s spectrum, (d) B1s spectrum, (e) N1s spectrum

The FT-IR spectra of the CQD and BNCQD sample are given in Figure S1 (see supporting information). Broad absorption band at 3100–3500 cm⁻¹ from BNCQD spectrum is assigned to O–H and N–H. Carbonyl C=O groups show an absorption band at approximately 1710 cm⁻¹. The hydrophilicity of BNCQD is achieved via the presence of these functional groups.³⁹ Two strong absorption peaks at 1432 and 1192 cm⁻¹ are attributed to B–O stretching vibration and B–C absorption band respectively and this is a strong evidence for the presence of B atom in the BNCQD structure. Two particular peaks at 1340 and 817 cm⁻¹ are observed, which are associated with the B–N bond stretching vibration and the B–N–B bending vibration, respectively and therefore the presence of N atom in structure is approved.

3.2. Optical Properties

Optical properties of obtained BNCQD were investigated using UV-Vis and Fluorescence techniques. Figure 4 shows the UV/Vis absorption spectrum and the PL spectra of BNCQD. Typical absorption peaks at 220 nm and 330 nm are observed which assigned to the π–π* transition of aromatic sp² domains and n–π* transition of functional groups on the BNCQD respectively.⁴⁰ As shown in Figure

4b, BNCQD exhibits an optimal emission peak at 503 nm under excitation at 400 nm, thus it shows a strong green light emission under PL irradiation. In addition, the fluorescence quantum yield (QY) of the resulted BNCQD was about 28.4% using quinine sulfate as the calculated standard reference.

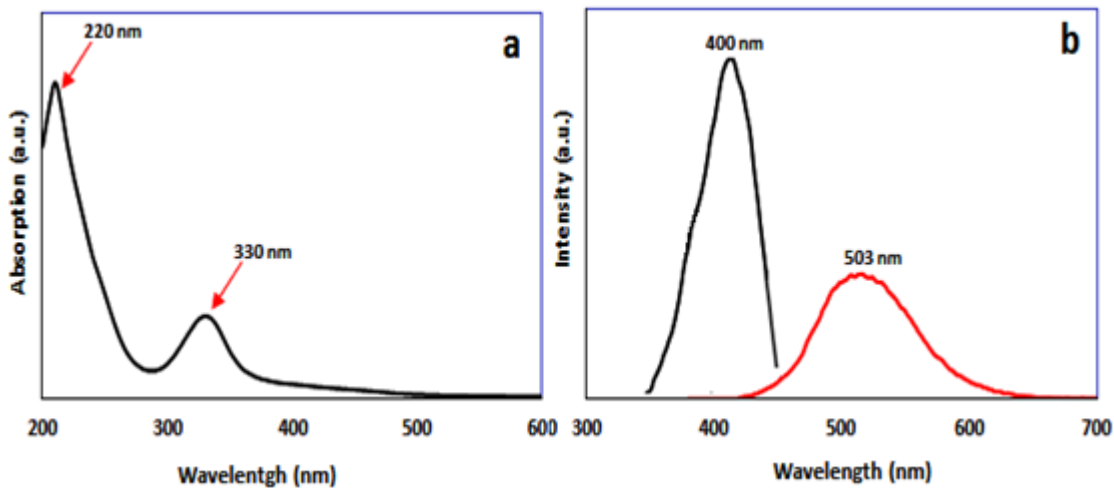


Figure 4. a) UV–vis absorption and b) PL spectra of the BNCQD: excitation (black), and emission (red)

3.3. Mechanism of Phosphate Ions Detection

For comparison of the effect of PO_4^{3-} on fluorescence of BNCQD and NCQD, the fluorescence spectra of these compounds are shown in the presence and absence of PO_4^{3-} in Figure 5. BNCQD shows a strong fluorescence emission peak at 503 nm, whereas NCQD (with quantum yield about 26.8) exhibit a weak emission peak at 503 nm and it results that fluorescence quantum yield of BNCQD is considerably higher than that of NCQD. It can be suggested that the coordination of carboxylate groups on the BNCQD surfaces to B atom in the structure of BNCQD leads to the formation of nonfluorescent BNCQD aggregates and decreasing of fluorescence. It is interesting to note that an obvious increase in fluorescence intensity of BNCQD is observed in the presence of PO_4^{3-} , whereas it has only a negligible influence on the fluorescence of NCQD.

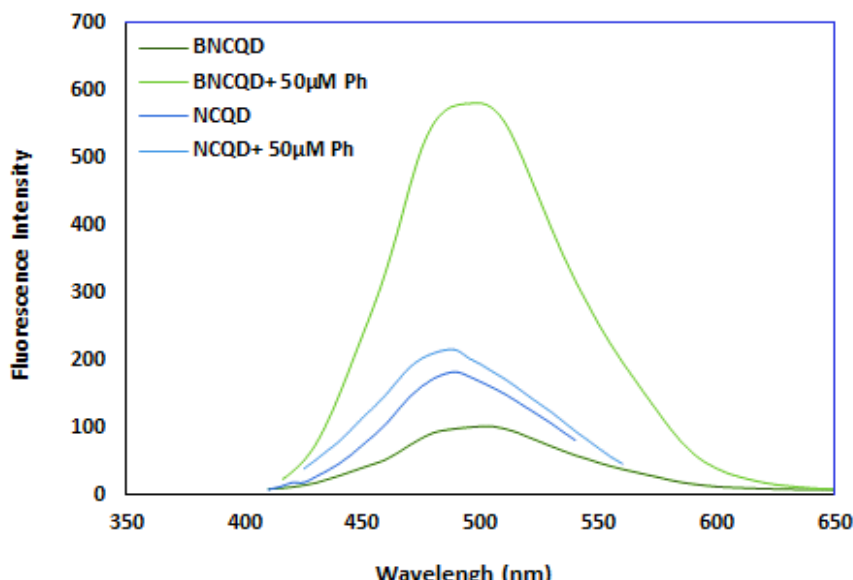


Figure 5. Fluorescence spectra of BNCQD and NCQD in the presence and absence of PO_4^{3-} .

The capability of a BNCQD sensing system towards the detection of PO_4^{3-} was evaluated by measuring the changes in fluorescence intensity of this compound at 503 nm with varying PO_4^{3-} concentration (Figure 6). It is clearly seen that BNCQD has a positive response towards PO_4^{3-} and the fluorescence intensity at 503 nm increases by the PO_4^{3-} concentration addition. As can be seen, the increasing in concentration of PO_4^{3-} from 0 to 120 μM leads an obvious enhancement in fluorescence intensity in the emission band at 503 nm. In fact, in the absence of phosphate ions, B^{3+} ions can coordinate with the carboxylate groups on the surface and doped nitrogen atoms in the carbon quantum dots, as a result, fluorescence of BNCQD are quenched through energy transfer or electron transfer processes.

In the present of PO_4^{3-} ions, they can donate their electron to vacancy orbitals of B atoms to create stable bonds and resulting increased fluorescence intensity of BNCQDs, again. Because B^{3+} ions exhibition a more tend to phosphor donor electron groups in PO_4^{3-} ions toward the oxygen in carboxylate groups and nitrogen of carbon dots. A linear relationship between the increased fluorescence intensity of BNCQDs and the concentration of PO_4^{3-} is observed (inset of Figure 6, 0.1 to 120 μM , $R^2 = 0.9989$ with the calibration equation is $\text{Y} = 2.4911 + 0.0479 [\text{PO}_4^{3-}]$). The limit of detection for phosphate ion was calculated to be 0.1 μM according to S_m equation which is comparable to the world health organization standard (0.2 μM) for drinking water.⁴¹

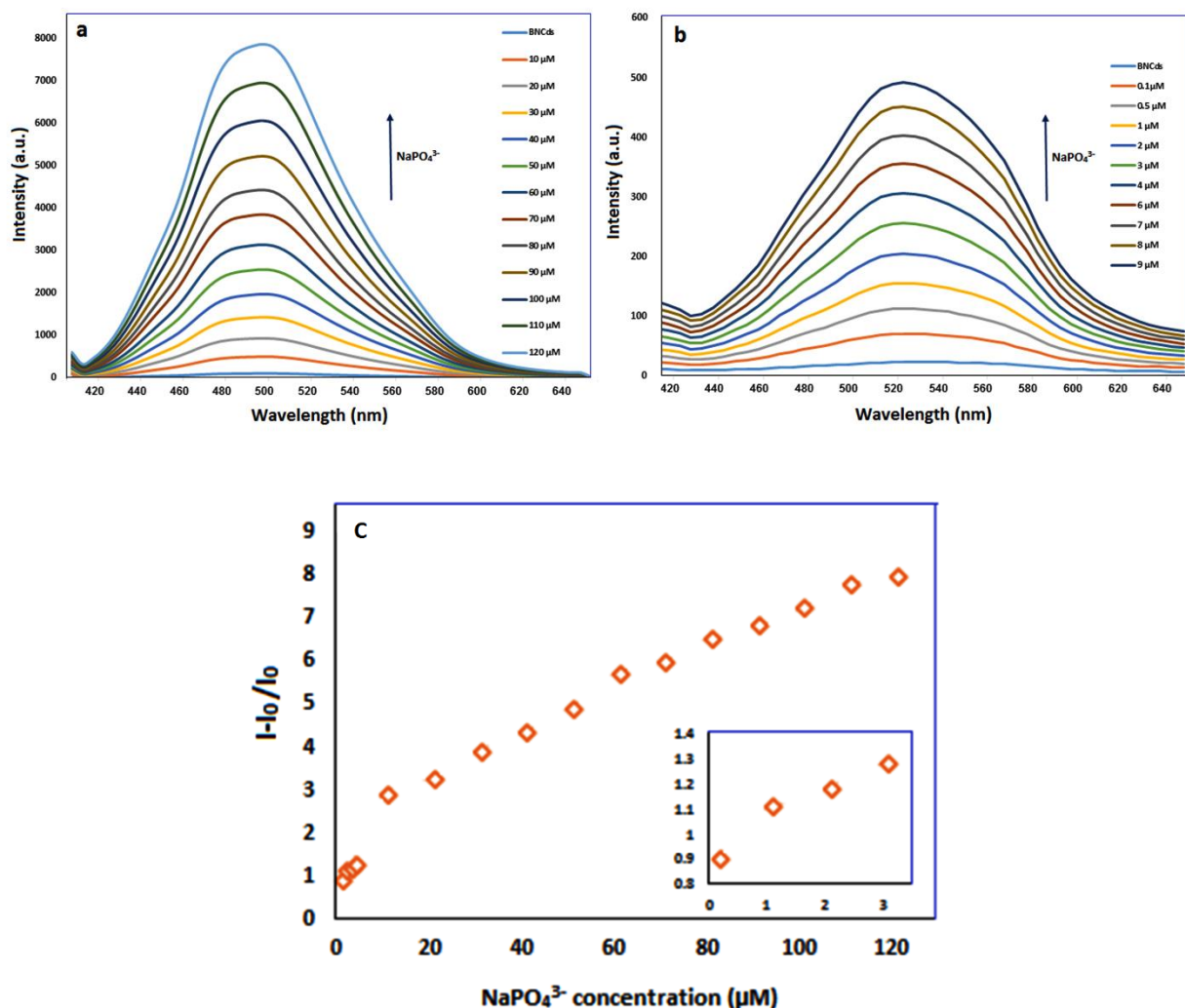


Figure 6. a and b) Fluorescence spectra of BNCQD aqueous solution upon addition of PO_4^{3-} in different concentrations at 400nm, **c)** Relationship between $(I - I_0)/I_0$ and PO_4^{3-} from 0.1 to 120 μM . I_0 and I are the PL intensities of BNCQD at 400 nm excitation in the absence and presence of PO_4^{3-} ions respectively.

To compare the selectivity of BNCQD against PO_4^{3-} ions, we perform titration with others anions. The selectivity of the fluorescent sensor for PO_4^{3-} over other substances such as CO_3^{2-} , NaOH and KOH was evaluated and the results are shown in Figure 8. As shown in Figure 7, no clear increase is observed with other ions in comparison with PO_4^{3-} which demonstrate high selectivity for PO_4^{3-} . Therefore, BNCQD can be introduced as an excellent sensitive and high specific sensor for PO_4^{3-} detection in real samples.

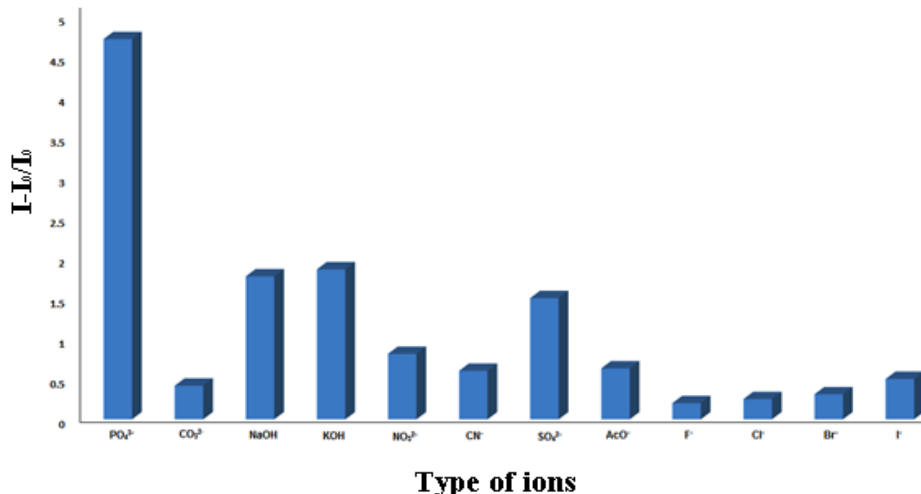


Figure 7. Selectivity of BNCQD towards PO_4^{3-} ion

4. Conclusion

In conclusion, we wish to introduce a specific, highly selective and rapid assay for the detection of PO_4^{3-} anion. Fluorescent B-doped carbon quantum dots is synthesized via a simple and one-pot MW-assisted method and is used as environmentally friendly and biocompatible sensor of PO_4^{3-} for the first time. The sensitivity is based on the coordination of PO_4^{3-} anion via its oxygen-donors to B atoms in the BNCQD structure. Fluorescence intensity of BNCQD is increased by the coordination of PO_4^{3-} . The fluorescence increasing efficiency is linearly correlated with the PO_4^{3-} concentration.

Acknowledgements

Financial support of this work by the research affairs of Azarbaijan Shahid Madani University is gratefully appreciated.

Supporting Information

Supporting information accompanies this paper on <http://www.acgpubs.org/journal/organic-communications>

ORCID

Azadeh Ostad Chinigar: [0000-0002-6963-2976](http://orcid.org/0000-0002-6963-2976)

Ashkan Shomali: [0000-0003-3085-4085](http://orcid.org/0000-0003-3085-4085)

Hassan Valizadeh: [0000-0002-8316-3221](http://orcid.org/0000-0002-8316-3221)

References

- [1] Lin, S. H.; Wu, C. L. Removal of nitrogenous compounds from aqueous solution by ozonation and ion exchange. *Water Res.* **1996**, *30*, 1851-1857.
- [2] Levine, S.; Schindler, D. Phosphorus, nitrogen, and carbon dynamics of Experimental Lake 303 during recovery from eutrophication. *Can. J. Fish. Aquat. Sci.* **1989**, *46*, 2-10.
- [3] De-Bashan, L. E.; Bashan, Y. Recent advances in removing phosphorus from wastewater and its future use as fertilizer. *Water Res.* **2004**, *38*, 4222-4246.
- [4] Almeelb,T. I; Bezbaruah, A. Aqueous phosphate removal using nanoscale zero-valent iron," in *Nanotechnology for Sustainable Development*. Springer, Cham, **2012**, 197-210
- [5] Kumar, M.; Badruzzaman, M.; Adham, S. Beneficial phosphate recovery from reverse osmosis (RO) concentrate of an integrated membrane system using polymeric ligand exchanger (PLE). *Water Res.* **2007**, *41*, 2211-2219.
- [6] Oehmen, A.; Lemos, P. C.; Carvalho, G.; Yuan, Z.; Keller, J. L.; Blackall, L.; Reis, M. A. Advances in enhanced biological phosphorus removal: from micro to macro scale. *Water Res.* **2007**, *41*, 2271-2300.
- [7] Zhang, G.; Liu, H.; Liu, R.; Qu, J. Removal of phosphate from water by a Fe–Mn binary oxide adsorbent. *J. Colloid Interfa. Sci.* **2009**, *335*, 168-174.
- [8] Gam M. X.; Liu, C. F.; Wu, Z. L.; Zeng, Q. L.; Yang, X. X.; Wu, W. B.; Li, Y. F.; Huang, C. Z. A surfactant-assisted redox hydrothermal route to prepare highly photoluminescent carbon quantum dots with aggregation-induced emission enhancement properties. *Chem. Commun.* **2013**, *49*, 8015-8017.
- [9] Liu, C.; Zhang, P.; Zhai, X.; Tian, F.; Li, W.; Yang, J.; Liu, Y.; Wang, H.; Wang, W.; Liu, W. Nano-carrier for gene delivery and bioimaging based on carbon dots with PEI-passivation enhanced fluorescence. *Biomaterials* **2012**, *33*, 3604-3613.
- [10] Jahan, S.; Mansoor, F.; Naz, S.; Lei, J.; Kanwal, S. Oxidative synthesis of highly fluorescent boron/nitrogen co-doped carbon nanodots enabling detection of photosensitizer and carcinogenic dye. *Anal. Chem.* **2013**, *85*, 10232-10239.
- [11] Das, G. S.; Tripathi, K. M.; Kumar, G.; Paul, S.; Mehara, S.; Bhowmik, S.; Pakhira, B.; Sarkar, S.; Roy, M.; Kim, T. Y. Nitrogen-doped fluorescent graphene nanosheets as visible-light-driven photocatalysts for dye degradation and selective sensing of ascorbic acid. *New J. Chem.* **2019**, *43*, 14575-14583.
- [12] Lu, F.; Zhou,Y.H.; Wu, L.H.; Qian, J.; Cao, S.; Deng, Y.F.; Chen, Y. Highly fluorescent Nitrogen-doped graphene quantum dots' synthesis and their applications as Fe (III) ions sensor. *Int. J. Opt.* **2019**, |Article ID 8724320, (9 pages).
- [13] Bai, J. M.; Zhang, L.; Liang, R. P.; Qiu, J. D. Graphene quantum dots combined with europium ions as photoluminescent probes for phosphate sensing. *Chem. Eur. J.* **2013**, *19*, 3822-3826.
- [14] Qin, J; Li, D; Miao, Y; Yan, G. Detection of phosphate based on phosphorescence of Mn doped ZnS quantum dots combined with cerium (iii). *R.S.C. Adv.* **2017**, *74*, 46657-46664.
- [15] Yan, D; He, Y; Ge, Y; Song, G. Fluorescent detection of phosphate in aqueous solution based on near infrared emission Ag2S QDs/metal–organic shell Composite. *J. Fluoresc.* **2017**, *1*, 227-233.
- [16] Dai, C; Yang, CX; Yan, X.P. Ratiometric fluorescent detection of phosphate in aqueous solution based on near infrared fluorescent silver nanoclusters/metal–organic shell composite. *Anal. Chem.* **2015**, *87*, 11455-11459.
- [17] Shomali, A.; Valizadeh, H.; Banan, A. Efficient synthesis of xanthene derivatives using carboxyl functionalized graphene quantum dots as an acidic nano-catalyst under microwave irradiation. *RSC. Adv.* **2015**, *5*, 88202-88208.
- [18] Valizadeh, H.; Shomali, A.; Nourshargh, S.; Mohammad-Rezaei, R. Carboxyl and nitrite functionalized graphene quantum dots as a highly active reagent and catalyst for rapid diazotization reaction and synthesis of azo-dyes under solvent-free conditions. *Dyes Pigments* **2015**, *113*, 522-528.
- [19] Shomali, A.; Valizadeh, H. Efficient Synthesis of Î± -Oximinoketones using carboxyl and nitrite functionalized graphene quantum dots: Dual role of nanostructure as a catalyst and reagent. *J. Adv. Chem.* **2016**, *12*, 4089-4096.
- [20] Baker, S. N.; Baker, G. A. Lumineszierende kohlenstoff-nanopunkte: Nanolichtquellen mit zukunft. *Angew. Chim.* **2010**, *122*, 6876-6896.
- [21] Shen J., Y. Zhu, X. Yang, J. Zong, C. Li, One-pot hydrothermal synthesis of graphene quantum dots surface-passivated by polyethylene glycol and their photoelectric conversion under near-infrared light. *Chem. Commun.* **2012**, *36*, 97-101.
- [22] Li, H.; Kang, Z.; Liu, Y.; Lee, S.T. Carbon nanodots: synthesis, properties and applications. *J. Mat. Chem.* **2012**, *22*, 24230-24253.

- [23] Sun, Y.-P.; Zhou, B.; Lin, Y.; Wang, W.; Fernando, K. S.; Pathak, P.; Meziani, M. J.; Harruff, B. A.; Wang, X.; Wang, vc BC9H. Quantum-sized carbon dots for bright and colorful photoluminescence. *J. Am. Chem. Soc.* **2006**, *128*, 7756-7757.
- [24] Jaiswal, A.; Ghosh, S. S.; Chattopadhyay, A. One step synthesis of C-dots by microwave mediated caramelization of poly (ethylene glycol). *Chem. Commun.* **2012**, *48*, 407-409.
- [25] Yang, Y.; Cui, J.; Zheng, M.; Hu, C.; Tan, S.; Xiao, Y.; Yang, Q.; Liu, Y.; One-step synthesis of amino-functionalized fluorescent carbon nanoparticles by hydrothermal carbonization of chitosan. *Chem. Commun.* **2012**, *48*, 380-382.
- [26] Qian, Z.S.; Ma, J.J.; Shan, X. Y.; Shao, L. X.; Zhou, L.; Chen, J. R.; Feng, H. Surface functionalization of graphene quantum dots with small organic molecules from photoluminescence modulation to bioimaging applications: an experimental and theoretical investigation. *R.S.C. Adv.* **2013**, *3*, 14571-14579.
- [27] Panchakarla, L. S.; Subrahmanyam, K. S.; Saha, S. K.; Govindaraj, A.; Krishnamurthy, H. R.; Waghmare, U. V.; Rao, C. N. R. Synthesis, structure, and properties of boron-and nitrogen-doped grapheme. *Adv. Mat.* **2009**, *21*, 4726-4730.
- [28] Subrahmanyam, K. S.; Panchakarla, L. S.; Govindaraj, A.; Rao, C. N. R. Simple method of preparing graphene flakes by an arc-discharge method. *J. Phys. Chem. C* **2009**, *113*, 4257-4259.
- [29] Sheng, Z.H.; Gao, H.L.; Bao, W.J.; Wang, F.B.; Xia, X.H. Synthesis of boron doped graphene for oxygen reduction reaction in fuel cells. *J. Mat. Chem.* **2012**, *22*, 390-395.
- [30] Wang, H.; Maiyalagan, T.; Wang, X. Review on recent progress in nitrogen-doped graphene: synthesis, characterization, and its potential applications. *ACS Catal.* **2012**, *2*, 781-794.
- [31] Marconcini, P.; Cresti, A.; Triozon, F.; Fiori, G.; Biel, B.; Niquet, Y.M.; Macucci, M.; Roche, S.; Atomistic boron-doped graphene field-effect transistors: a route toward unipolar characteristics. *ACS Nano.* **2012**, *6*, 7942-7947.
- [32] Yang, Y.; Cui, J.; Zheng, M.g.; Hu, C.; Tan, S.; Xiao, Y.; Yang, Q.; Liu, Y. One-step synthesis of amino-functionalized fluorescent carbon nanoparticles by hydrothermal carbonization of chitosan. *Chem. Commun.* **2012**, *48*, 380-382.
- [33] Zhai, X. Y.; Zhang, P.; Liu, C. J.; Bai, T.; Li, W. C.; Dai, L.; Liu, W. G. Highly luminescent carbon nanodots by microwave-assisted pyrolysis. *Chem. Commun.* **2012**, *48*, 7955-7957.
- [34] Xu, Y.; Wu, M.; Liu, Y.; Feng, X. Z.; Yin, X. B.; He, X. W.; Zhang, Y. K. Nitrogen-doped carbon dots: A facile and general preparation method, photoluminescence investigation, and imaging applications. *Chem. Eur. J.* **2013**, *19*, 2276-2283.
- [35] Zheng, A. X.; Cong, Z. X.; Wang, J. R.; Li, J.; Yang, H. H.; Chen, G. N. Highly-efficient peroxidase-like catalytic activity of graphene dots for biosensing. *Biosens. Bioelectron.* **2013**, *49*, 519-524.
- [36] Ryther, H.; Dunstan, W. M. Nitrogen, phosphorus, and eutrophication in the coastal marine environment. *Science* **1971**, *171*, 1008 –1013.
- [37] Gupta, V.; Chaudhary, N.; Srivastava,; Sharma, R. G. D.; Bhardwaj, R.; Chand, S. Luminscent graphene quantum dots for organic photovoltaic devices. *J. Am. Chem. Soc.* **2011**, *133*, 9960.
- [38] Wu, J. S.; Pisula, W.; Mullen, K.; Graphenes as potential material for electronics. *Chem. Rev.* **2007**, *107*, 718-747.
- [39] Qu, S.; Wang, X.; Lu, Q.; Liu, X.; Wang, L. A. A biocompatible fluorescent ink based on water-soluble luminescent carbon nanodots. *Angew Chem. Int. Ed.* **2012**, *51*, 12215–12218.
- [40] Pan, D.; Zhang, J.; Li, Z.; Wu, C.; Yan, X.; Wu, M. Observation of pH-, solvent-, spin-, and excitation-dependent blue photoluminescence from carbon nanoparticles. *Chem. Commun.* **2010**, *46*, 3681–3683.
- [41] Brown, R. M.; McClell, N. I.; Deininger, R. A.; Tozer, R. G. A Water quality index: Do we dare? *Water Sew. Work.* **1970**, *117*, 339-343.

A C G
publications

© 2020 ACG Publications